Methyl substituents at the 11 or 12 position of retinal profoundly and differentially affect photochemistry and signalling activity of rhodopsin

Verhoeven, M.A.; Bovee-Geurts, P.H.M.; Groot, H.J.M. de; Lugtenburg, J.; Grip, W.J. de

doi:10.1016/j.jmb.2006.07.039 J. Mol. Biol. (2006) 363, 98–113

JMB

Available online at www.sciencedirect.com

ScienceDirect

ELSEVIER

Methyl Substituents at the 11 or 12 Position of Retinal Profoundly and Differentially Affect Photochemistry and Signalling Activity of Rhodopsin

Michiel A. Verhoeven[1], Petra H. M. Bovee-Geurts[2] Huub J. M. de Groot[1], Johan Lugtenburg[1] and Willem J. DeGrip[1,2]*

[1]*Leiden Institute of Chemistry Leiden University, P.O. Box 9502, 2300 RA Leiden The Netherlands*

[2]*Department of Biochemistry Nijmegen Center for Molecular Life Sciences, Radboud University Nijmegen Medical Center, P.O. Box 9101, 6500 HB Nijmegen, The Netherlands*

**Corresponding author*

The C-11=C-12 double bond of the retinylidene chromophore of rhodopsin holds a central position in its light-induced photoisomerization and hence the photosensory function of this visual pigment. To probe the local environment of the HC-11=C-12H element we have prepared the 11-methyl and 12-methyl derivatives of 11-Z retinal and incorporated these into opsin to generate the rhodopsin analogs 11-methyl and 12-methyl rhodopsin. These analog pigments form with much slower kinetics and lower efficiency than the native pigment. The initial photochemistry and the signaling activity of the analog pigments were investigated by UV-vis and FTIR spectroscopy, and by a G protein activation assay. Our data indicate that the ultrafast formation of the first photointermediate is strongly perturbed by the presence of an 11-methyl substituent, but much less by a 12-methyl substituent. These results support the current concept of the mechanism of the primary photoisomerization event in rhodopsin. An important stronghold of this concept is an out-of-plane movement of the C-12H element, which is facilitated by torsion as well as extended positive charge delocalization into the C-10–C-13 segment of the chromophore. We argue that this mechanism is maintained principally with a methyl substituent at C-12.

In addition, we show that both an 11-methyl and a 12-methyl substitutent perturb the photointermediate cascade and finally yield a low-activity state of the receptor. The 11-methyl pigment retains about 30% of the G protein activation rate of native rhodopsin, while the 12-methyl chromophore behaves like an inverse agonist up to at least 20 °C, trapping the protein in a perturbed Meta-I-like conformation.

We conclude that the isomerization region of the chromophore and the spatial structure of the binding site are finely tuned, in order to achieve a high photosensory potential with an efficient pathway to a high-activity state.

Keywords: rhodopsin analog pigment; retinal synthesis; quantum yield; photoactivation; fourier-transform infrared spectroscopy

Introduction

Rhodopsin is the G protein-coupled photoreceptor protein in the retina of vertebrates that initiates the visual transduction cascade in dim light vision.[1,2] Rhodopsin contains a protonated 11-Z retinylidene Schiff base in its active site, which functions as an inverse agonist. The protein binds this ligand in the 12-s-*trans* conformation and the non-bonding interactions between the C-13 methyl group and the C-10 hydrogen atom give rise to a

Present address: M.A. Verhoeven, High Field NMR Laboratory, Institut de Chimie des Substances Naturelles, 1 Avenue de la Terrasse, 91190 Gif-sur-Yvette, France.

Abbreviations used: Meta, metarhodopsin; Batho, bathorhodopsin; FTIR, Fourier transform infrared spectroscopy; HOOP, hydrogen-out-of-plane.

E-mail address of the corresponding author: wdegrip@oase.uci.ru.nl

non-planar structure.[3–5] The resulting torsions in the chromophore configure the polyene tail for fast photoisomerization around the C-11=C-12 double bond.[3,6,7] Within 1 ps following light absorption, the primary photoproduct bathorhodopsin (Batho) is formed, which contains a highly strained protonated all-E retinylidene Schiff base in the active site.[8–11] Subsequent thermal steps lead within milliseconds to the signaling intermediate metarhodopsin-II (Meta-II), which contains a relaxed unprotonated all-E retinylidene Schiff base in the active site that acts as a full agonist.[1,2,12] Studies on rhodopsin analogs without the 9-methyl or 13-methyl group (C-19, C-20) have established that these methyl groups contribute significantly to the propagation of the photochemical cascade leading to the signaling state of the protein.[13–22] For example, the absence of the 13-methyl group leads to a significantly lower quantum yield of $\Phi = 0.47$ compared to $\Phi = 0.65$ for native rhodopsin, while upon light absorption by 9-desmethyl rhodopsin, the active state 9-desmethyl Meta-II is generated with much lower efficiency.

Chemical modification of the isomerization region of the 11-Z retinylidene moiety (C-10••C-13) can help to provide insight into the structural basis of the high rate and efficiency of the photochemical reaction.[23,24] Earlier studies have pursued the effect of an additional methyl group at the 10 position.[4,23,25] For instance, it was observed that 10-methyl rhodopsin has a lower quantum yield ($\Phi = 0.55$) than the native system ($\Phi = 0.65$), and that thermal conversion of the first photoproduct (Batho) to the next intermediate is shifted to a higher temperature. An additive effect is observed upon simultaneous removal of the 13-methyl group yielding 10-methyl-13-desmethyl rhodopsin, which shows a further reduction in quantum yield to $\Phi = 0.35$.[13]

In this study, the effect of methyl substitution at the C-11 and C-12 position of retinal (Scheme 1) is investigated. In earlier work, the corresponding rhodopsin analog pigments were generated in low yield and only the value of λ_{max} was reported.[26,27] It was claimed very recently that a methyl group at position C-12 would downshift the pK_a of the Meta-I ↔ Meta-II equilibrium, which should result in strongly reduced signalling activity of 12-methyl rhodopsin at physiological pH.[22]

We have improved the efficiency of the chemical synthesis of 11-methyl and 12-methyl retinal significantly, as well as the production of the corresponding rhodopsin analogs. The photochemical and signalling activity of the 11-methyl and 12-methyl rhodopsin analogs have been studied by means of UV-vis and Fourier transform infrared (FTIR) spectroscopy and a G protein binding assay. The aim of this study is to resolve and understand the details of the ligand–receptor communication and photoactivation in the native pigment. The results indicate mixed effects of methyl group insertion at positions C-11 or C-12 on: (i) protein–ligand interaction as well as at two stages in the photosequence; (ii) the primary photoisomerization step; and (iii) the signaling activity of the receptor at the final stage.

Results and Discussion

The use of modified retinal derivatives allows us to investigate ligand–protein interactions, the photoisomerization process and, finally, the effect of substituents on the mechanisms leading to the signaling activity of the visual receptor rhodopsin. First, the efficiency and rate of binding, and the spectral properties of the retinal analog in the binding site provide information about ligand–

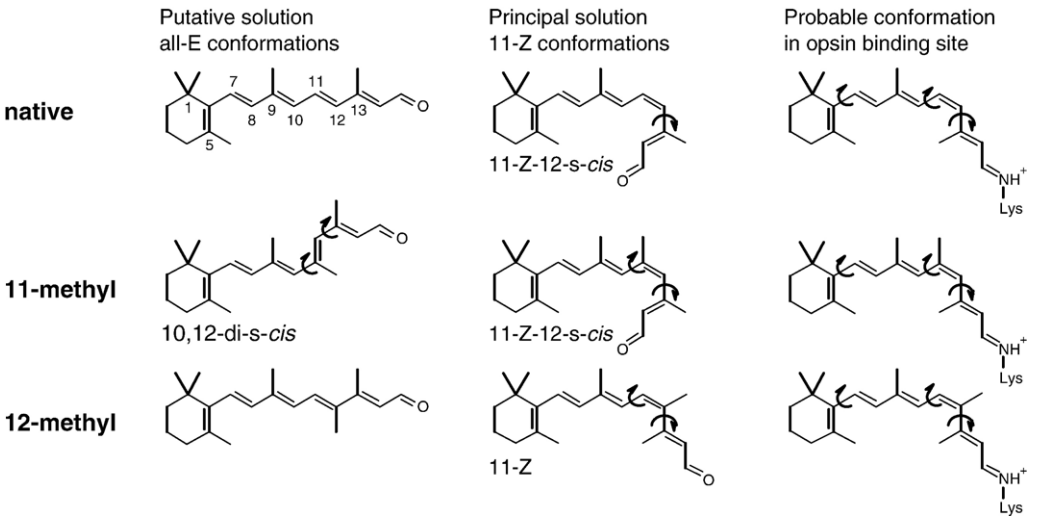

Scheme 1. Principal solution conformations of the 11-Z retinal derivatives used in this study determined by NOE NMR spectroscopy (middle column). For comparison, the putative all-E solution structures are shown in the left-hand column, and the probable conformation in the opsin binding site is shown in the right-hand column. The arrows indicate bond torsion that occurs due to intramolecular steric repulsion.

protein interactions and binding site constraints in the ground state. Steric crowding in the binding site will affect the binding rate and efficiency, and may lead to distortion of the chromophore in the binding site. Second, photoisomerization, the primary step in photoactivation of rhodopsin, transforms the 11-Z retinylidene ligand into a strained all-E conformation. In this ultrafast process (<200 fs) the shape of the protein-binding pocket, fitted to accommodate the 11-Z configuration of the chromophore, is essentially preserved. This restrains the relaxation of the chromophore, leading to pronounced torsions in the primary photoproduct.[8,9,11,28–30] The protein subsequently transforms from the inactive to the active form, which is triggered by the relaxation of conformational energy (~32 kcal/mol) that is stored in the strained chromophore during Batho formation.[31–35] Third, in contrast to the primary event, further receptor activation involves changes in the protein structure that require a much longer time-scale (up to ~1 ms).[2,12,30,36,37] There is abundant evidence that all three processes are differentially sensitive to the presence of a methyl substituent at C-9, C-10 and/or C-13.[14–16,18–24,38] Here, this picture is complemented by analyzing the effects of methyl substituents at C-11 or C-12. Conformational transitions representing the formation of the primary photoproduct and the putative signaling state are probed by vibrational spectroscopy. A functional parameter of the photoisomerization process is presented in the quantum yield, while photochemical transitions and G protein activation are used in a functional characterization of formation of the active signaling state.

11-Methyl retinal

In Figure 1(a) the UV-visible spectrum for 11-Z 11-methyl retinal in hexane is presented (continuous line). The spectrum of 11-Z retinal is given for comparison in Figure 1(e) (continuous line). The relatively strong side band at 250 nm in 11-Z retinal compared to the main (α) band at 363 nm (Figure 1(e)) reflects the preference of free retinal

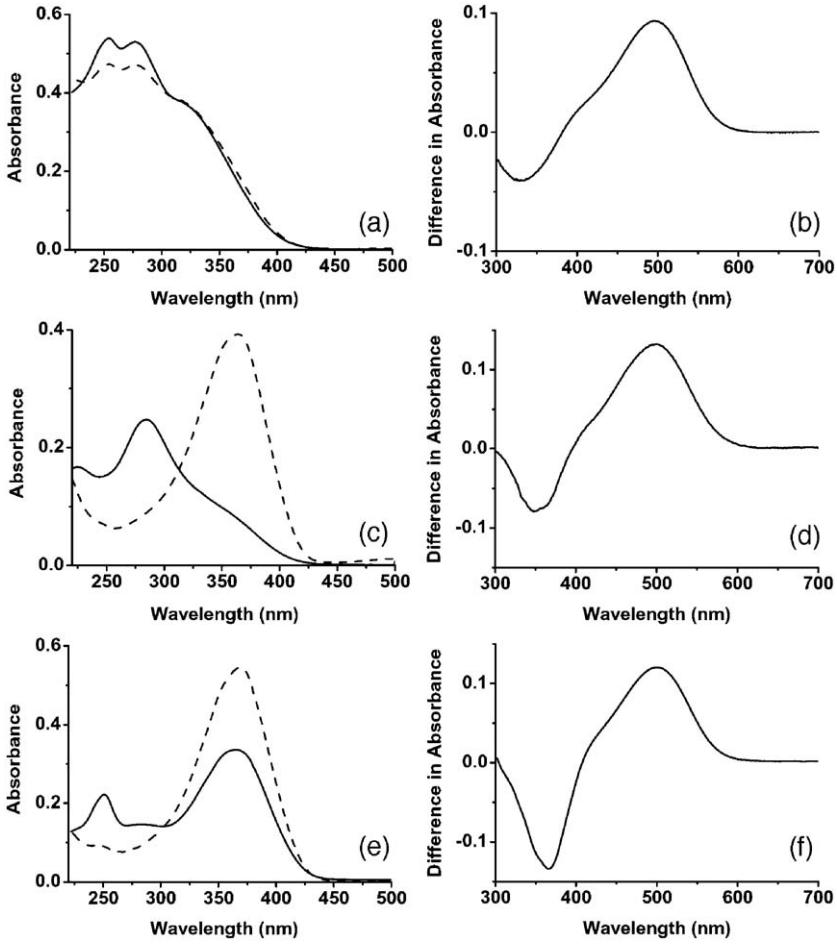

Figure 1. Spectral properties of native 11-Z, 11-Z 11-methyl, and 11-Z 12-methyl retinal and corresponding rhodopsin pigments. (a), (c) and (e) UV-visible spectra are shown of (a) 11-Z 11-methyl, (c) 11-Z 12-methyl and (e) 11-Z retinal in hexane before (continuous line) and after illumination in the presence of iodine (broken line). (b), (d) and (f) UV-visible difference spectra of the corresponding rhodopsin pigments, prepared from opsin and the 11-Z retinals, yielding (b) 11-methyl rhodopsin, (d) 12-methyl rhodopsin and (f) native rhodopsin. The difference spectra were obtained by subtracting the spectrum after illumination from the dark-state spectrum (not shown) as outlined in Materials and Methods.

for a twisted 12-s-*cis* conformation due to steric hindrance between the C-10 carbon atom and the 13-methyl group (Scheme 1). Such hindrance is relieved upon isomerization to the 11-E configuration. This is evident in the spectrum obtained after photoisomerization in the presence of trace amounts of iodine (Figure 1(e), broken line). This spectrum represents a mixture with predominantly the relaxed all-E and some 13-Z isomer, and shows a strong reduction of the side band with a strong increase in the α band. In the 11-Z 11-methyl analog, the intensity of the α band is strongly reduced in favor of side bands at 250 nm and 280 nm, suggesting additional torsion in this analog around the C-10–C-11 bond due to steric repulsion between the methyl groups at C-9 and C-11 (Scheme 1).[39,40]

In contrast to the strong absorbance band at 380 nm and low side band intensity in the photoequilibrated state of native retinal (Figure 1(e)), illumination of 11-Z 11-methyl retinal does not lead to major changes (Figure 1(a), broken line). This indicates that the thermodynamically most favorable conformation of 11-methyl retinal also has a distorted polyene backbone. NMR analysis of all-E 11-methyl retinal in $CDCl_3$ indeed showed that this molecule has a distorted 10,12-di-s-*cis* conformation in order to avoid intramolecular hindrance of adjacent methyl groups (Scheme 1).[41]

11-Methyl rhodopsin

Ligand–protein interaction

The difference spectrum for 11-methyl rhodopsin obtained by subtracting the spectrum after illumination from the dark-state spectrum in a micellar solution (not shown) is presented in Figure 1(b). This yields an absorbance maximum at 496(±2) nm (Table 1). The incorporation of this ligand is at least 100-fold slower than that of native 11-Z retinal, and the incorporation efficiency is only 54(±5) % (Table 1). The absorbance maximum agrees with an earlier note by Liu *et al.* (498 nm).[27] Previously, we discussed the possibility that low regeneration rates at higher molar retinal analog to opsin ratios could lead to blockade of the entry site and low efficiencies of regeneration.[42] Our results with both 11-methyl and 12-methyl retinal (see below) support this idea.

It is generally accepted that the rhodopsin-binding pocket requires a ligand that has the 10,12-di-s-*trans* conformation (Scheme 1).[27,43] The quite similar spectral properties of native and 11-methyl rhodopsin lead to the conclusion that this conformation is adopted by 11-methyl retinal in the binding pocket. Nevertheless, significant torsion is expected around the C-10–C-11 bond to accommodate the methyl groups at C-9 and C-11.[41] On the basis of the X-ray structure of rhodopsin,[5,43] the additional 11-methyl group might experience steric interaction with protein residues in the E2 loop and in helix II. Such steric effects could explain the low rate of regeneration. A structurally more restricted analog, 11-Z 11,19-ethano retinal, was reported to generate the corresponding analog pigment efficiently.[44,45] The ethano bridge renders this ligand sterically less demanding, since it restricts the mobility of the C-9–C-11 segment and eliminates the repulsive interaction between the 9-methyl and 11-methyl groups. In fact, the formation rate of the early photointermediates of the 11,19-ethano pigment is very similar to that of rhodopsin.[44]

It is concluded that the 11-methyl analog of 11-Z retinal does not optimally fit into the binding site. Steric hindrance is expected with residues of the E2 loop and of helix II. Nevertheless, it generates a pigment that is stable towards detergent solubilization and 10 mM hydroxylamine at ambient temperature and physiological pH.

Table 1. Regeneration efficiencies and λ_{max} values of the pigments used in this study

Retinal derivative	Regeneration rate relative to rhodopsin	Regeneration efficiency (% of rhodopsin)	λ_{max} (nm)
Native 11-Z	≡1	≡100	498±1
11- Z 11-Methyl	<0.01	54±5	496±2
11-Z 12-Methyl	<0.004	37±10	500±2

Standard deviations are given for $n=3$–5.

Photoisomerization

Figure 2 shows the FTIR difference spectrum for photoproduct formation of the native and modified pigments at 80 K. In native rhodopsin, illumination at this temperature generates the Batho intermediate.[1] The negative signals in these spectra correspond with vibrations of the pigment that change in frequency or intensity, or disappear upon transition into the all-E photoproduct, while the positive peaks are characteristic for the photoproduct. The peaks in the region 1800–1550 cm^{-1} represent changes in the protein, while below 1550 cm^{-1} the major changes relate to the chromophore.[30,36,46–48] For the native state, most of the bands in the difference spectrum can be attributed to specific vibrations in the retinylidene backbone. Most prominent are C=C and C=N stretches in the range 1500–1600 cm^{-1}, C–C stretches in the range 1100–1300 cm^{-1}, and wag vibrations below 1050 cm^{-1}.[30,49,50] The most striking difference between the natural Batho and the 11-methyl photoproduct is the absence of any distinct hydrogen-out-of-plane (HOOP) wags in the latter in the 800–1100 cm^{-1} region (Figure 2, middle trace). The presence of the 11-methyl group will affect HOOP vibrations related to the C-11 carbon and the C-10–C-11=C-12 segment. For instance, the weak rhodopsin vibration at 969 cm^{-1} assigned to coupled C-11H and C-12H wags and the strong band at 921 cm^{-1} in Batho that is assigned to the isolated C-11H wag[49,50] are absent from the 11-methyl analog. However, the 875 cm^{-1}, 854 cm^{-1}, 848 $cm^{-1}$and 838 cm^{-1} Batho bands assigned to the wags of C-10H, C-12H, C-14H and C-7H=C-8H, respectively,[50] are also either

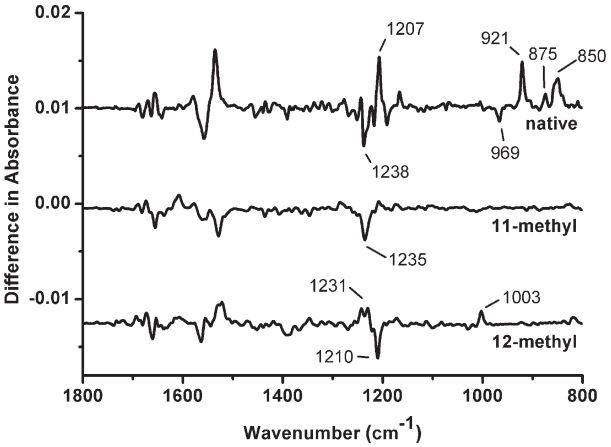

Figure 2. FTIR difference spectra of native, 11-methyl and 12-methyl rhodopsin after illumination at 80 K. In native rhodopsin, illumination at this temperature generates the Batho intermediate.[1] Difference spectra were constructed by subtracting the dark-state spectrum from the spectrum after illumination. Negative peaks represent vibrational bands characteristic for the dark state, positive peaks vibrational bands characteristic for the photoproduct.

attenuated strongly or entirely absent from the analog. In the C–C stretch region, the strong vibration at 1207 cm^{-1}, assigned to the C-14–C-15 stretch in native Batho,[49] is absent, while the band at 1238 cm^{-1} in rhodopsin, which reflects reorientation of the C-12–C-13 bond after isomerization, is replaced by a broad band at 1235 cm^{-1} in 11-methyl rhodopsin. This possibly represents the C-12–C-13 and the C-10–C-11 vibrations, the latter being upshifted from 1096 cm^{-1} in rhodopsin by the presence of the 11-methyl group.[13]

Photoreversal of Batho (λ_{max} = 540 nm) to rhodopsin can be achieved by illumination of the photoproduct with $\lambda > 610$ nm light,[1] but no reversal is observed for the 11-methyl photoproduct with either $\lambda > 610$ nm or $\lambda > 530$ nm light (not shown). One explanation could be that, in contrast to native rhodopsin, the electronic spectrum of 11-methylrhodopsin and its primary photoproduct strongly overlap. The downshift in frequency of the C=C stretch vibration around 1550 cm^{-1} accompanying the rhodopsin to Batho transition (Figure 2, upper trace) reflects this red-shift of the electronic absorbance band.[8,47] There is no clear shift in the C=C band pattern of the 11-methyl difference spectrum (Figure 2, middle trace), which would agree with only minor changes in spectral properties between 11-methylrhodopsin and its primary photoproduct. So far, we could not obtain reproducible spectral data by UV/vis cryospectroscopy to confirm this interpretation. The loss of red-shift in the 11-methyl photoproduct could indicate a different distribution of the torsional strain in the all-E polyene as compared to the native Batho due to steric interaction between the adjacent methyl groups (Scheme 1) and/or stronger steric crowding with protein residues. This might result in additional torsion around single bonds, which would counteract a red shift and attenuate HOOP intensities.

The quantum yield of 11-methyl rhodopsin relative to native rhodopsin was determined according to equation (2) by measuring the time-dependent decrease in the main band absorbance recorded under continuous low-bleaching conditions, yielding a value of $\Phi = 0.28(\pm 0.04)$ (Table 2), considerably less than the $\Phi = 0.65$ of rhodopsin. Since the quantum yield is a measure for the transition rate of the excited state to the photoproduct,[8,13,50] the additional methyl group and associated conformational constraints apparently decrease this transition rate significantly. This would agree with a differentially strained all-E chromophore in the 11-methyl photoproduct with less torsion in the C-11=C-12 and C-13=C-14 moieties. This can be compared with 13-desmethyl Batho, which is formed with a quantum yield of $\Phi = 0.47$,[13] where the HOOP vibrations are also strongly attenuated.[14,51]

Signaling activity

Figure 3 shows a UV-vis spectral analysis of late phototransitions at 10 °C in membrane suspensions of 11-methyl rhodopsin at pH 6.5 and native rhodopsin at pH 6.0. For native rhodopsin membranes, an equilibrium mixture of Meta-I (λ_{max} = 480 nm) and Meta-II (λ_{max} = 380 nm) is generated within milliseconds, the composition of which depends on the pH and the temperature.[2,52,53] Under the experimental conditions (pH < pK_a, see below), this mixture consists mainly of the active signaling state Meta-II (Figure 3(c), dash-dot trace; Figure 3(d), continuous trace). Subsequently, Meta-II decays slowly with release of all-E retinal (λ_{max} = 380 nm) from the binding pocket under formation of opsin and *N*-retinylidene opsin (λ_{max} = 360 nm in the unprotonated form and ~445 nm in the protonated form).[54] The formation of protonated *N*-retinylidene opsin is apparent from the increase of absorbance at ~450 nm (Figure 3(c)), and in the difference of the spectra taken 10 s and 40 min after illumination (Figure 3(d), dotted line). Subsequent addition of

Table 2. Quantum yields and relative transducin activation rates for (des)methyl rhodopsin analog pigments

Rhodopsin derivative	Quantum yield Φ	Transducin activation rate (% native rhodopsin)[a]
Native	0.65[b]	≡100
11-Methyl	0.28±0.04	29±1
12-Methyl	0.54±0.08	6±4
11-Methyl, 13-desmethyl	0.18±0.04	70±3
10-Methyl	0.55[c]	35±5
13-Desmethyl	0.44±0.05	53±29

[a] $n = 4$.
[b] From Kim *et al.*[67]
[c] From DeLange *et al.*[23]

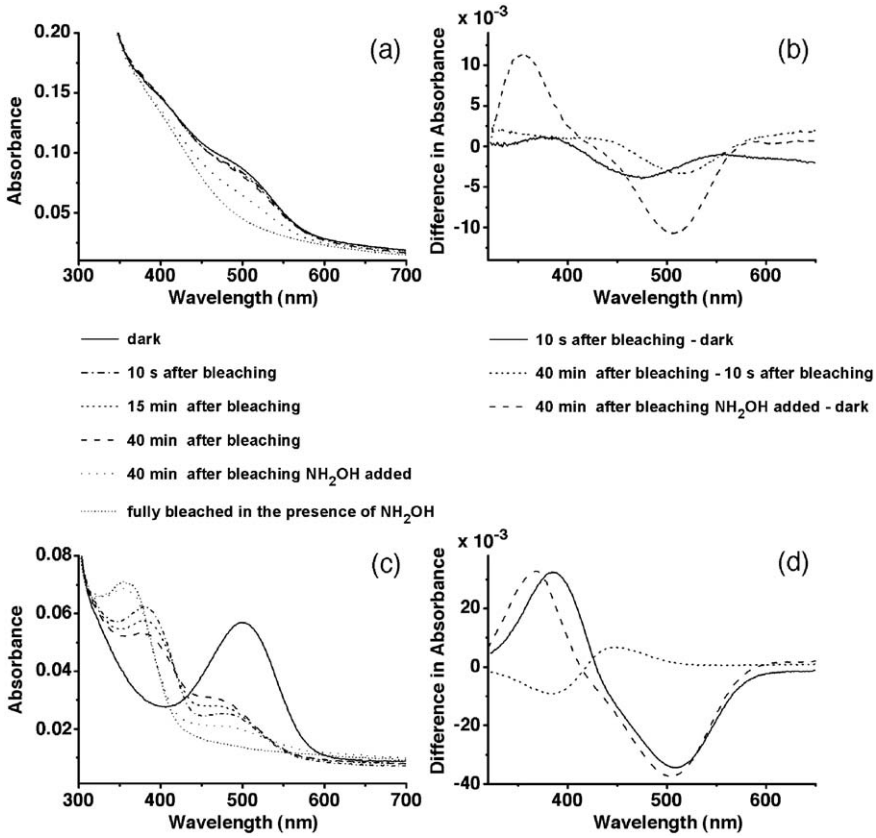

Figure 3. Spectral analysis of the late photoreactions at 10 °C in membrane suspensions of (a) and (b) 11-methyl rhodopsin at pH 6.5, and (c) and (d) native rhodopsin at pH 6.0. (a) and (c) show the raw spectra, (b) and (d) present difference spectra between relevant steps.

hydroxylamine converts all photoproducts into retinoxime (λ_{max}=365 nm) and shows that most of the bleached pigment (negative peak around 500 nm in Figure 3(d)) indeed produced Meta-II.

The 11-methyl rhodopsin absorbance (continuous line in Figure 3(a)) is superimposed on a large background of a scattering signal that is especially apparent in the fully bleached spectrum (densely dotted line). This background originates in the high concentration and size diversity of the proteoliposome population. A Meta-II-like photointermediate of 11-methyl rhodopsin forms inefficiently at 10 °C and pH 6.5. This is illustrated by the very modest increase of the absorbance around 380 nm and the small decrease of the absorbance around 500 nm, even 40 min after illumination, in

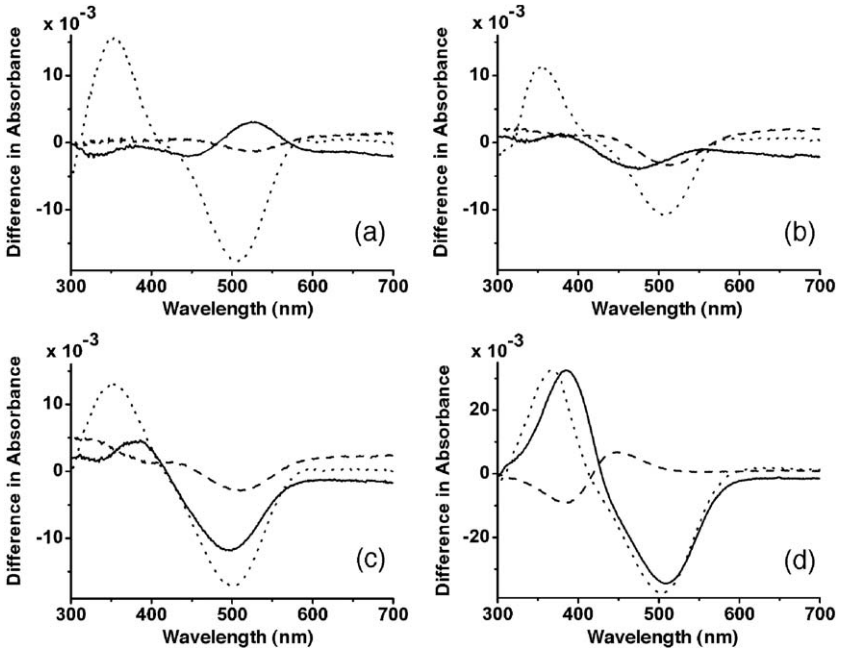

Figure 4. The pH-dependence of the 11-methyl rhodopsin photocascade. UV-visible difference spectra are shown at (a) pH 7.5, (b) 6.5 and (c) 5.5, and (d) as a reference for native rhodopsin at pH 6.0, recorded at 10 °C in membrane suspensions. Continuous lines represent difference spectra between 10 s after illumination and the dark state, broken lines between 40 min and 10 s after illumination, and dotted lines between subsequent addition of hydroxylamine and the dark state.

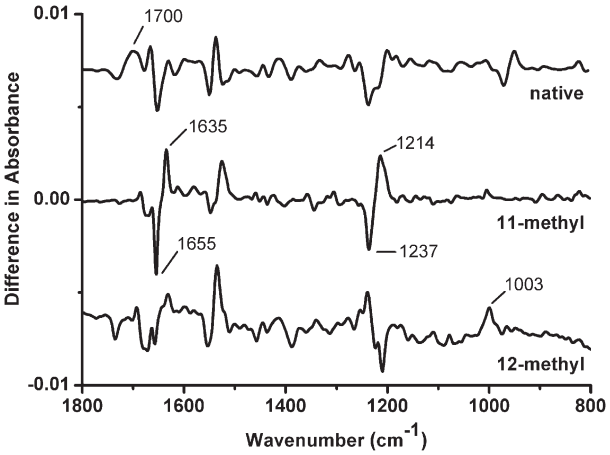

Figure 5. FTIR difference spectra of native, 11-methyl and 12-methyl rhodopsin after illumination at 253 K. In native rhodopsin, illumination at this temperature generates the meta-I intermediate.[1,2,30] Difference spectra were constructed by subtracting the dark-state spectrum from the spectrum after illumination. Negative peaks represent vibrational bands characteristic for the dark state, positive peaks represent vibrational bands characteristic for the photoproduct.

spite of the fact that addition of hydroxylamine demonstrates that at least 50% of the pigment was photo-activated (Figure 3(a), dotted line; Figure 3(b), broken line).

Illumination of rhodopsin results in an equilibrium of Meta-I and Meta-II that is pH-dependent,[1,2,52,53,55] with a pK_a of about 6.8 at 10 °C and at pH 8.5 yields predominantly the meta-I intermediate, which decays slowly into Meta-III.[56] We investigated whether the photocascade of the 11-methyl pigment was also dependent on pH. Figure 4 shows difference spectra at 10 °C for 11-methyl rhodopsin illuminated at pH 7.5, pH 6.5 and pH 5.5 and for native rhodopsin at pH 6.0 as a reference. The spectra from rhodopsin (Figure 4(d)) show the photoconversion of rhodopsin to a mixture of about 88% Meta-II and about 12% Meta-I (continuous trace) and the decay of Meta-II into *N*-retinylidene opsin (broken trace). The data obtained with 11-methyl rhodopsin clearly show pH-dependence. At pH 7.5, this pigment is largely photoconverted into a very slowly decaying intermediate absorbing around 520 nm (Figure 4(a), continuous trace). This intermediate might represent an 11-methyl Meta-I analog that is strongly red-shifted from the native Meta-I. Alternatively, it might represent the Lumi analog, the precursor of Meta-I that absorbs at 504 nm in the native state. In that case, the native Meta-I↔Meta-II equilibrium would have been perturbed by the presence of the 11-methyl group into a Lumi↔Meta-I/II equilibrium. Upon lowering the pH, the proportion of a product at about 380 nm increases (Figure 4(b) and (c), continuous traces). This slowly decays and probably reflects the 11-methyl Meta-II intermediate. These results suggest that the signaling state of 11-methyl rhodopsin is formed less efficiently as compared to native rhodopsin.

Figures 5 and 6 show FTIR difference spectra recorded at a temperature where in the native system the rhodopsin→Meta-I and the rhodopsin→Meta-II transitions can be probed, that is −20 °C and 10 °C, respectively. The 11-methyl rhodopsin difference spectrum at −20 °C (Figure 5, middle trace) clearly deviates from the native state. Sharp peaks at 1655 cm^{-1} and 1635 cm^{-1} and the absence of the broad band at 1700 cm^{-1} strongly resemble the Lumi transition of native rhodopsin.[30,36] This corroborates the evidence from the UV-visible data that formation of the late intermediates is hindered in this analog pigment. Relatively strong bands at 1237 cm^{-1} and 1214 cm^{-1} in the 11-methyl difference spectrum derive from single-bond C–C vibrational changes that probably reflect the different vibrational pattern of the twisted 11-Z and all-E 11-methyl polyene.

The native rhodopsin→Meta-II transition is characterized by a specific band pattern that reflect changes in the protein structure.[36] Representative are, for instance, signals at 1767 cm^{-1}, 1750 cm^{-1}, 1710 cm^{-1}, 1640 cm^{-1}, 1437 cm^{-1} and 1391 cm^{-1} (Figure 6, upper trace). The difference spectrum for 11-methyl rhodopsin (Figure 6, middle trace) also shows these features of Meta-II clearly, but they are markedly attenuated, signifying reduced formation of a Meta-II like intermediate under these conditions (10 °C, pH range 5.5–6.0). This result agrees with the less efficient formation of the Meta-II like intermediate for 11-methyl rhodopsin observed with UV-vis spectroscopy. The bilobal band at 1237 cm^{-1} and 1214 cm^{-1} is still significant in the 11-methyl spectrum and may reflect the presence of earlier intermediates next to Meta-II.

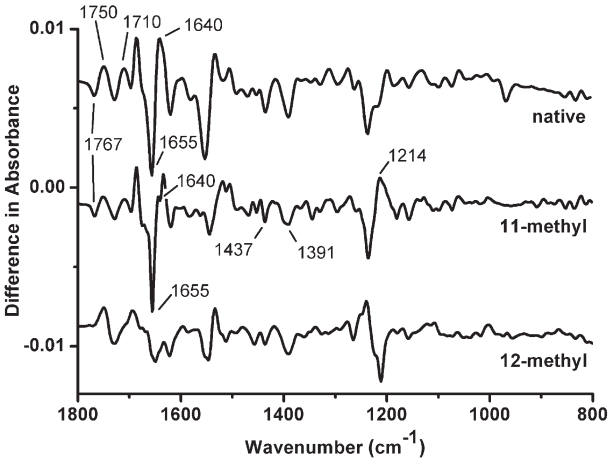

Figure 6. FTIR difference spectra of native, 11-methyl and 12-methyl rhodopsin after illumination at 10 °C. In native rhodopsin, illumination at this temperature and this approximate pH of 5.5–6.0. generates almost a full equivalent of the meta-II intermediate.[1,2,30] Difference spectra were constructed by subtracting the dark-state spectrum from the spectrum after illumination. Negative peaks represent vibrational bands characteristic for the dark state, positive peaks represent vibrational bands characteristic for the photoproduct.

In line with these spectral observations, the transducin activation rate by 11-methyl rhodopsin is reduced strongly, to only 29% of that by rhodopsin (Table 2). This indicates that the all-E 11-methyl retinylidene ligand is only a partial agonist for receptor activation, comparable to, for instance, the 10-methyl analog,[23] and other ring and polyene modifications.[18,22,38,57,58] The picture that emerges from these results is that the inefficient formation of late intermediates up to Meta-II results in inefficient activation of the G-protein. The altered temperature-dependence of the photocascade transitions in 10-methyl and 11-methyl rhodopsin suggests an increase in the activation enthalpy for formation of Meta-II. This is most likely due to steric interaction between the additional methyl group of the ligand and the protein environment. This would corroborate recent inferences that translational repositioning of the ligand is required up to the final stage of receptor activation, the formation of Meta-II.[59–61] In that case, we would expect that removal of the 13-methyl group would relieve steric perturbation and attenuate the effect of the 11-methyl group. Indeed, we find for 11-methyl 13-desmethyl rhodopsin an increased efficiency in Meta-II formation and an increase in transducin activation rate to about 70% of that of native rhodopsin (Table 1).[62]

12-Methyl retinal

The UV/visible spectrum of 11-Z 12-methyl retinal in hexane shows a main absorbance band at 285 nm, which, upon illumination in the presence of traces of iodine, shifts to a strong band at 365 nm (Figure 1 (c)). In the 11-Z 12-methyl analog, the intensity of the α band around 350 nm is reduced strongly in favor of the side band at 285 nm. Our NMR data indicate that the C-12–C-13 bond has an s-*trans* configuration, which must be due to steric repulsion between the adjacent methyl groups at C-12 and C-13. To relieve the consequent steric interaction between the C-10H and C-13-methyl substituents, the molecule probably adopts twists around the C-10–C-11 and C-12–C-13 bonds (Scheme 1). This is in obvious contrast to 11-Z retinal, which adopts a more relaxed 12-s-*cis* conformation in solution. The spectrum produced upon photoisomerization (Figure 1(b), broken trace) very much resembles that of the native situation (Figure 1(e), broken trace). This agrees with formation of the all-E 12-methyl isomer, which does not suffer from steric interactions between the polyene methyl groups and can adopt a fully relaxed conformation similar to native all-E retinal (Scheme 1).

12-Methyl rhodopsin

Ligand–protein interaction

Figure 1(d) shows the difference spectrum for 12-methyl rhodopsin obtained by subtracting the spectrum after illumination from the dark-state spectrum. This yields an absorbance maximum at 500(±2) nm (Figure 1; Table 1). The incorporation rate of 11-Z 12-methyl retinal is at least 200-fold smaller than that of native 11-Z retinal, and the incorporation efficiency is only 37(±10)% (Table 1). The absorbance maximum is comparable with an earlier estimate of 495 nm by Liu *et al*,[26] but those authors achieved hardly any pigment formation (maximally 5%). Quite recently, Vogel *et al*.[22] reported high regeneration efficiencies for 11-Z 12-methylretinal with an absorbance maximum for the resulting pigment of 487 nm. The reason for this discrepancy is not known. In five independent experiments we obtained considerable variation in regeneration efficiency, but it did not reach a high level (25–45%), while the absorbance maximum was always within the range 498–502 nm.

The quite similar spectral properties of native and 12-methyl rhodopsin (Figure 1) allow the conclusion that 11-Z 12-methyl retinal also adopts the 10,12-di-s-*trans* conformation in the binding pocket (Scheme 1). This would not deviate much from the free conformation, and therefore the very low regeneration rate is probably due to a poor fit in the binding pocket. On the basis of the X-ray structure of rhodopsin,[5,43] and derived analyses,[9,63] the additional 12-methyl group would experience steric crowding with several protein residues, primarily Cys187, and with the H-bonding network comprising Tyr268, Glu181, Ser186 and Wat2a. In fact, the 12-methyl pigment is not very stable against nucleophilic attack on the Schiff base by hydroxylamine unless kept at a low temperature (≤10 °C), which is another indication of steric strain in the binding pocket.

Photoisomerization

The FTIR analysis of first photoproduct formation of 12-methyl rhodopsin is presented in Figure 2 (bottom trace). Similar to 11-methyl rhodopsin, the 12-methyl rhodopsin photoproduct does not show any of the characteristic HOOP vibrations of the native Batho, while it presents a new signal at 1003 cm^{-1}. We assign this signal tentatively to the 12-methyl wag vibration.[8,47] This may have obtained stronger IR-activity as a result of the out-of-plane movement of the 12-methyl group upon isomerization, and closer interaction with the protein environment, in particular Trp265.[9,11,63] The C=C signal around 1550 cm^{-1} shows a bilobal shape similar to that of the native state, suggesting that, like the native Batho, the 12-methyl photoproduct has a red-shifted absorbance band. Indeed, like the native system, the 12-methyl photoproduct can be photoreversed by illumination with light λ>610 nm (data not shown). The C–C vibrational difference pattern of the 12-methyl pigment is quite different from that of the native state as well as from that of the 11-methyl pigment. It is expected that the methyl group at position 12 will upshift the C-12–C-13 stretch vibration, which is the major contributor

to the signal at 1238 cm^{-1} in native rhodopsin.[49] Hence, the 12-methyl C–C fingerprint pattern is difficult to interpret without further information.

From the analysis of the time-dependent decrease of the main absorbance band under low-bleaching conditions, the quantum yield for 12-methyl rhodopsin photoisomerization is estimated as $\Phi = 0.54(\pm 0.08)$, which is not much smaller than the $\Phi = 0.65$ of native rhodopsin, and significantly larger than the $\Phi = 0.28(\pm 0.04)$ of 11-methylrhodopsin. Hence, compared to 11-methyl rhodopsin, the photoisomerization process of 12-methyl rhodopsin closely resembles that of native rhodopsin. This is discussed below in more detail.

Signaling activity

The late photocascade of 12-methyl rhodopsin at 10 °C and pH 6.5 (Figure 7) shows a slowly decaying intermediate at 477 nm, that most likely represents a 12-methyl Meta-I-like intermediate. The difference spectrum directly after illumination (Figure 7(b), continuous line) is very similar to that obtained for rhodopsin at pH 8.0, which corresponds to the transition to Meta-I.[23,53] Similar results are observed for 12-methyl rhodopsin at pH 7.5 and pH 5.5 (not shown). This suggests that at 10 °C and pH > 5.5, the dark reactions of 12-methyl rhodopsin proceed to a Meta-I-like stage that decays slowly with the release of retinal (Figure 7(b), dotted line). This agrees with the data presented by Vogel *et al*.,[22] who calculated a pK_a of 4.7 for the Meta-I ↔ Meta-II transition of the 12-methyl pigment at 0 °C.

To investigate the behavior of the 12-methyl Meta-I-like intermediate at different temperatures, photolysis was performed at 20 °C and at 30 °C at pH 6.5 (Figure 8). The behavior at 10 °C and at 20 °C is very similar and indicates exclusive formation of a slowly decaying Meta-I-like intermediate. At 30 °C, a more complex behavior is observed, with a Meta-I like intermediate decaying more rapidly into Meta-II and Meta-III-like intermediates and free retinal. These observations are basically confirmed by vibrational analysis (Figures 5 and 6, bottom trace). Except for the protein region between 1650 cm^{-1} and 1800 cm^{-1}, the 12-methyl rhodopsin difference spectrum at −20 °C (Figure 5) shows many features of the native rhodopsin→Meta-I transition. The similarity below 1600 cm^{-1} of the FTIR difference spectra of 12-methyl rhodopsin recorded at either −20 °C or at 10 °C (Figures 5 and 6) is striking, and indicates that only minor structural changes in the 12-methyl chromophore occur after raising the temperature beyond the threshold for native Meta-II formation. The signal at 1003 cm^{-1} is reduced in intensity, probably reflecting more conformational freedom of the 12-methyl group at 10 °C. The protein region (1600–1800 cm^{-1}) does show additional features at 10 °C compared to −20 °C, but differs strongly from that of native Meta-II (Figure 6). The bilobal band feature at 1767(−) cm^{-1} and 1750(+) cm^{-1} that is indicative of H-bonding changes in protein residue Asp83 upon Meta-II formation, is absent. Also, the signal at 1710 cm^{-1} indicative of protonation of Glu113 is not observed. The 12-methyl spectra show an additional feature at 1694 cm^{-1}, observed also by Vogel *et al*,[22] that might reflect a change in a Gln or Asn side-chain or in backbone structure. These observations suggest that the 12-methyl chromophore can proceed to a Meta-I-like conformation but blocks rearrangements in the binding site required to proceed to an active Meta-II state. In line with these results, the G protein activation rate of the 12-methyl pigment at 20 °C is only 6% of that of native rhodopsin (Table 2) and not significantly different from the intrinsic activity (4 (±2)%) of the apoprotein opsin in the presence of all-E retinal.[2,23] Apparently, at room temperature and below, the 12-methyl ligand efficiently "locks" the protein in a Meta-I-like conformation and the rate of transducin activation becomes very small. Hydrolysis of the Schiff base linkage with release of the ligand on the minute time-scale eventually results in the apoprotein with a low level of intrinsic activity. This behavior is clearly reminiscent of an inverse agonist. Therefore, the 11-Z as well as the all-E

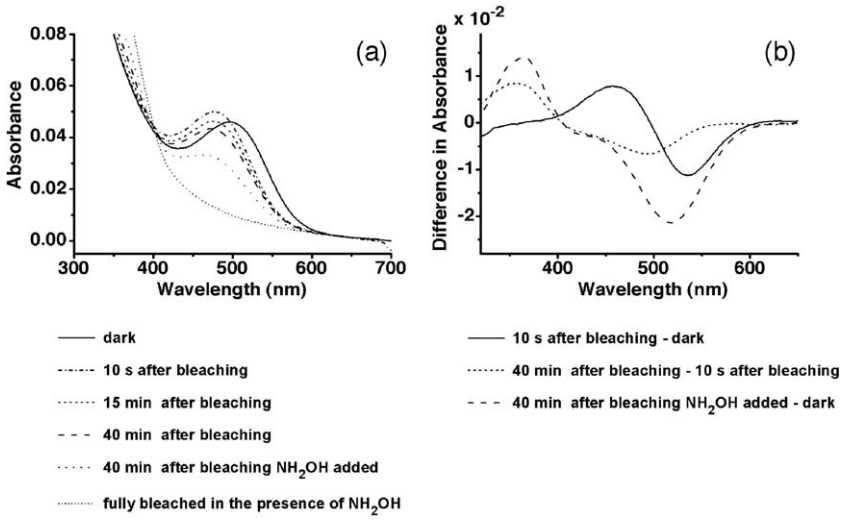

Figure 7. Late stage of the photocascade of 12-methyl rhodopsin at 10 °C and pH 6.5. (a) UV-vis spectra of 12-methyl rhodopsin in the dark and at different intervals after illumination, with subsequent addition of hydroxylamine. (b) Difference spectra between relevant steps.

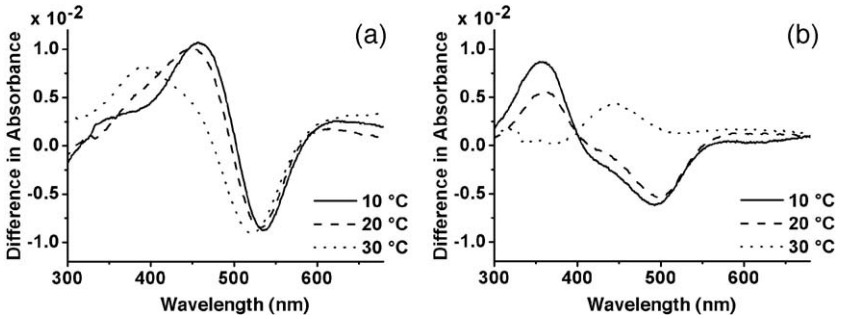

Figure 8. UV-visible difference spectra for 12-methyl rhodopsin at 10 °C, 20 °C and 30 °C, and pH 6.5. (a) Difference between the absorbance spectrum measured 10 s after illumination and the dark spectrum. (b) Difference between the absorbance spectrum measured 20 min after illumination and the spectrum 10 s after illumination.

configuration of 12-methyl retinal can be classified as an inverse agonist for opsin.

Compilation

A large body of literature shows that studying artificial pigments using modified retinals can provide elementary insight into the mechanism and structure–function relationships of visual pigments. In this study, we focus on the central part of the polyene that is essential for the photochemical isomerization reaction converting the 11-Z configuration of the ligand into all-E, and we present spectroscopic and biochemical data of opsin regenerated with 11-Z 11-methyl and 11-Z 12-methyl retinal. To our knowledge, this is the first study addressing this vital segment of the ligand in such detail. Methyl substitution at either the C-11 or the C-12 position has remarkably mixed effects on the regeneration efficiency, the generation of photointermediates and the G protein activation properties. The relatively low to moderate level of incorporation of these derivatives reflects the tight packing of the retinylidene moiety in the opsin-binding pocket, in this case particularly the isomerisation region that is in close contact with the E2 loop. Apparently, the tolerance of the binding pocket for an additional 10-methyl, 11-methyl or 12-methyl group is low, but removal of the 13-methyl group can partially compensate for this effect by allowing more flexibility in the terminal section of the polyene.[13,62] The 10-methyl, 11-methyl and 12-methyl pigments all exhibit perturbation of the photocascade transitions, resulting in inhibition or less efficient formation of the active state Meta-II. This shows that small steric modifications can lead to ligand–protein contacts that hamper relaxation of the retinylidene and protein structure towards the spatial position of the fully activated receptor. In addition, our data demonstrate that minor repositioning of a substituent can shift the ligand class from partial agonist to inverse agonist. Our results support earlier evidence that formation of the activated receptor requires selective rearrangement of the ligand. Since the Meta-I → Meta-II transition is entropy-driven,[34,64] additional protein–ligand steric contacts appear to impose an enthalpy threshold that delays or inhibits the native activation pathway.

The photoisomerization mechanism of native rhodopsin has been the subject of many experimental and theoretical studies.[6–10,28] It is suggested that the mechanism underlying the efficient isomerization of the retinylidene group in the excited state of rhodopsin involves the expansion of the C=C double bonds and simultaneous displacement of the hydrogen atoms in the C-11H=C-12H motif from a *cis* to a *trans* position with respect to each other. For native rhodopsin, the main displacement would be a rotation at the site of the C-12H element in the chromophore,[6,9,10] which agrees with the observation that the locked 11,19-ethano rhodopsin analog shows normal photointermediate kinetics,[44] and with the recently published crystal structure of Batho.[11] It has been suggested that a prerequisite for an efficient isomerization is a steep and coherent path over the excited state surface, and that the speed and efficiency are correlated closely.[7,8,10,13] Since with 500 nm light we find the efficiency of the primary step in the photoreaction of 12-methyl rhodopsin ($\Phi = 0.54$) not much reduced compared to that of native rhodopsin ($\Phi = 0.65$), this would imply that the 12-methyl group in 12-methyl rhodopsin performs an out-of-plane movement comparable to the trajectory of the C-12 hydrogen in rhodopsin. Energetically, this seems plausible, considering the following simplified calculation based upon Newtonian dynamics. To achieve the angular momentum allowing the hydrogen atom at C-12 in rhodopsin to rotate over an angle of about 110° in about 200 fs to arrive at the first C-11=C-12 transoid intermediate photorhodopsin,[10] about 0.1 kcal mol^{-1} of energy is required.[65] To realize the same rate for a methyl group at C-12 would increase the energy demand to about 4 kcal mol^{-1}. Contributions by vibrational motion and by restrictions of the binding pocket will be mutually counteractive and are neglected. From the incident photon energy (~57 kcal mol^{-1} at 500 nm) about 32 kcal is stored in the first stable ground-state photoproduct Batho.[35,66] At wavelengths smaller than 520 nm (~55 kcal.mol^{-1}) the quantum yield for rhodopsin is essentially invariant.[67] Thus, at 500 nm there should be at least 2 kcal mol^{-1} surplus energy, which would suffice to drive a 12-methyl group towards a transoid position in 250–300 fs. This would correspond to a quantum yield in the range 0.5–0.6,[13] in agreement with our data. Although this is a crude calculation, it implies clearly that a methyl group

at C-12 need not markedly disturb the native photoisomerization process. We anticipate that heavier groups would strongly reduce the rate and quantum yield of photoisomerization. For instance, based upon the same calculation, a 12-bromo substituent would require about 30 kcal mol^{-1} to achieve a 110° rotation in 200 fs.

The intriguing observation remains that a methyl group at C11 leads to a strong reduction in the quantum yield. We attribute this to internal steric crowding in the retinal polyene moiety that will affect the initial molecular conformation in the dark state, but becomes particularly prominent when approaching the all-E configuration.[41] The ground state and Batho structures would indicate steric interaction between the C-9 and C-11 methyl groups and the C-11- and C-13 methyl groups, respectively.[11] This will modify the energy surface of the isomerization path. Connecting the C-9 and C-11 methyl groups, as in 11,19-ethano retinal,[44,45] releases a major element of this crowding perturbation yielding a ground-state and an excited-state structure that is closer to the native system. In addition, the unfavorable effect of energy dissipation by molecular motion of this segment is expected to be significantly less for the 11,19-ethano pigment than for 11-methyl rhodopsin. Although a quantum yield has not been determined, this might at least explain the rather normal early photointermediate kinetics observed for 11,19-ethanorhodopsin.[44]

In conclusion, our study completes a series of studies investigating the effect on photoactivation of rhodopsin of a single addition or removal of a methyl group at positions in the central, photoactive segment, C-9–C-14, of the chromophore. First of all, the important conclusion can be drawn that all available data, including those obtained upon methylation of C12, do concur with an out-of-plane movement of the =C12 substituent as the primary mechanism of the photoisomerization process. On the other hand, it is remarkable that every single modification perturbs the photoactivation process at the early stage, as indicated by a reduction in quantum yield, as well as at the late stage, as indicated by a reduction in signaling activity. In some cases, this effect can be partially rescued by a second modification, usually removal of the 13-methyl group. It is obvious that the steric properties of the ligand and the binding pocket have become finely tuned, combining a high photosensory potential, with an efficient production of the high-activity state. Most modifications generate a ligand that retains at least partial agonist activity (demethylation at C-9 or C-13, methylation at C-10 or C-11) up to full agonist activity (methylation at C-14) in the all-E configuration. In contrast, methylation at C-12 eliminates all agonist activity. Obviously, minor structural modification can drastically modify the functional characteristics of a ligand. This is in line with a growing body of evidence in the G protein coupled receptor field, that subtle structural changes may pull a ligand over the entire range of activities, from full agonist to full inverse agonist. This emphasizes the need of very accurate mapping of *in situ* ligand structure and ligand–protein contacts to allow rational drug design of ligands with preselected activity.

Materials and Methods

Synthesis of 11-methyl and 12-methyl retinal

All syntheses were performed *via* Wittig and Horner-Wadsworth-Emmons strategies that are generally used for retinoids and carotenoids.[68,69] Since photoisomerization of all-E 11-methyl retinal into the 11-Z isomer is very inefficient, a stereoselective synthetic route was developed. Synthesis of 11-Z 11-methyl retinal was done in the dark by condensation of (β-ionylidene prop-2-yl) triphenylphosphonium bromide and 3-cyano-2-methyl-propa-2-enal in refluxing 1-butene oxide. The Wittig salt is prepared from β-ionylidene acetaldehyde,[70] by reduction of the aldehyde function with methyl lithium and conversion of the resulting secondary alcohol to the phosphonium salt as described.[71] The aldehyde is made from the previously described acetal,[72] by acidic deprotection of the acetal in 2% (v/v) phosphoric acid at 60 °C. Reduction of the retinonitrile with diisobutylaluminiumhydride (DIBAl-H) gives all-E and 11-Z isomers that can be separated by column chromatography (silica with diethylether: petroleum ether 20/80 (v/v) as eluent). Synthesis of 11-methyl-13-desmethyl retinal is accomplished by condensation of β-ionylidene phosphonium bromide[71] and aldehyde 5-methyl-6-oxo-hexa-2,4-dienoic ethyl ester in refluxing 1-butene oxide. The latter aldehyde is prepared from 4-(diethylphosphono) buta-2-enoic ethyl ester[73] and 1,1-dimethoxy acetone with subsequent deprotection of the acetal. Reduction of the retinoic ester to the alcohol by titration with at least 2 equivalents of DIBAl-H in dry petroleum ether and oxidation of the alcohol with MnO_2 in dichloromethane gives a mixture of retinal isomers. This mixture is enriched in the 9-Z and 11-Z isomers by irradiation in acetonitrile and the isomers are subsequently isolated by HPLC.[69] Synthesis of 12-methyl retinal is accomplished by reaction of β-ionylidene acetaldehyde with 2-(diethyl phosphono) propanoic ethyl ester,[74] and subsequent conversion of the ester to the methyl ketone by reaction with methyl lithium in the presence of trimethylsilylchloride at −100 °C.[75] Aqueous work-up yields the methyl ketone that is converted to 12-methyl retinal by reaction with diethylphosphono acetonitrile and subsequent reduction with DIBAl-H. After irradiation, the 11-Z isomer is isolated by HPLC separation.[69] The 9-Z 12-methyl retinal isomer was present as a minor component of, presumably, the 13-Z fraction. Scheme 1 illustrates the principal solution structures of the compounds used in this study determined by 2-D NOE NMR spectroscopy, which was used to identify the 11-Z isomer unequivocally. UV-visible absorbance spectra of the retinal analogs were recorded in hexane solution. The λ_{max} of the main absorbance band and the overall absorbance profile of the ligand, including the intensities of the accessory bands contain information about torsions in the polyene.[39] Addition of a dilute iodine solution to the retinal solution and subsequent

illumination for 60 s was used to establish a photo-equilibrium containing the thermodynamically most favorable configurations, usually with a preponderance of the all-E and 13-Z isomers.[76]

Generation of rhodopsin analogs

Bovine rod outer segment membranes in the opsin form (opsin membranes) were prepared from fresh, light-adapted eyes.[77] The regeneration capacity of these preparations was estimated from the A_{500}/A_{280} ratio that is obtained after incubation with a threefold excess of 11-Z retinal. A ratio of 2.0 represents membranes in which the opsin-binding site is saturated with ligand. The opsin membranes that were used showed a regeneration capacity in the range of 90–100% for native 11-Z retinal. All manipulations were performed under dim red light ($\lambda > 610$ nm; Schott RG610 long-pass filter) and the incubation was performed in an inert argon atmosphere. Opsin membranes were suspended in buffer A (20 mM Pipes (pH 6.5), 130 mM NaCl, 4 mM KCl, 2 mM $CaCl_2$, 0.1 mM EDTA, 1 mM dithioerythritol), to a final concentration of opsin of about 50 μM. Aliquots of two- to threefold molar excess of retinal or retinal derivative were added in a small volume of dimethylformamide (≤4% (v/v) final volume) with 12 hour intervals until pigment formation had leveled. The pigment analogs were incubated for at least 12 h and up to 48 h with up to ten equivalents of retinal derivative. The extent of pigment formation was assessed after every 12 h of incubation by measuring the spectral increase at 530 nm. After incorporation had leveled, the amount of unregenerated opsin remaining was assessed in a small test sample from the incubation vessel from the additional amount of rhodopsin formed upon addition of one equivalent of 11-Z retinal. The total absorbance of pigment that was finally obtained in this sample was always within 10% of the control value. Hence, the molar extinction coefficients of the analog pigments match that of rhodopsin and were taken as 40,000(±4000) $M^{-1}cm^{-1}$. To remove the excess of retinal analog, this usually is converted into the corresponding oxime by addition of hydroxylamine to a concentration of 10 mM, and subsequently two extractions are performed with 50 mM heptakis-(2,6-di-*O*-methyl)-β-cyclodextrin (Aldrich),[23] followed by washing twice with doubly distilled water. This procedure was followed for 11-methyl rhodopsin, but no hydroxylamine was used for 12-methyl rhodopsin, since it reacts slowly with the bound ligand, and only a single extraction step with cyclodextrin was performed. If a native lipid/protein ratio needed to be restored, the pigments were solubilised in 20 mM nonyl-1-β-glucoside in buffer A and mixed with a 50-fold molar excess of Asolectin (Sigma), a crude soybean lipid extract containing a mixture of natural phospholipids. Reconstitution in proteoliposomes was accomplished by centrifugation through a discontinuous sucrose gradient.[78] The resulting pigment membranes were washed with doubly distilled water and stored at −80 °C under argon in light-tight containers.

Spectral analysis of the rhodopsin analogs and of photo-intermediate formation

The wavelength of maximum absorbance (λ_{max}) for rhodopsin and for the analog pigments was determined in a mixed micellar solution with 10 mM hydroxylamine and 20 mM dodecyl-1-β-maltoside in buffer A as corresponding to the peak position in the difference spectrum obtained by subtracting the spectrum after 300 s illumination (Schott GG430 long-pass filter) from the dark-state spectrum.

Spectral analysis of photo-intermediate formation was performed on pigment membranes suspended in buffer A to a final concentration of 1 μM pigment using a Perkin-Elmer Lambda 18 double-beam spectrometer equipped with an end-on photomultiplier detector. A circulating waterbath was used to control the sample temperature. The sample was bleached for 10 s using a Schott OG530 long-pass filter and subsequent spectra were recorded after selected time-intervals. Addition of hydroxylamine to 20 mM then converts all photo-intermediates from Batho through Meta-III, as well as free retinal into the corresponding oxime that absorbs at ~365 nm. The difference spectrum after addition of hydroxylamine gives an indication of the total amount of bleached pigment, since the oxime has no significant absorption at 500 nm. Subsequent illumination in the presence of hydroxylamine fully bleaches the pigment and gives an indication of the total amount of pigment in the sample.

Photosensitivity of pigments

The photoisomerization quantum yields of the analog pigments were determined relative to that of rhodopsin ($\Phi_{Rho} = 0.65$) or of isorhodopsin ($\Phi_{Iso} = 0.27$) that are well characterized experimentally.[13,67,79] Pigments were solubilised in buffer A with 10 mM dodecyl-1-β-maltoside and 10 mM hydroxylamine to give an absorbance at 500 nm of about 0.16. Solutions were kept at 10 °C and illuminated through a 504(±5) nm or 497(±10) nm interference filter (Schott). The illumination conditions were such that the halftime of pigment bleaching was between 20 min and 60 min. Spectra were taken during 2 h with intervals of 5–10 min. The halftime of the pigment absorbance decay in the dark, which provides a measure of pigment stability, was >20 h. The slope S of a straight line through A_f–log (10^{A_t}–10^{A_f}) is a measure of the photosensitivity $\varepsilon\Phi$.[23,79] In this expression, A_t denotes the absorbance at a selected wavelength after time t, and A_f is the absorbance after complete bleaching. Comparison of the slopes gives the quantum yield of the pigment analogue (Φ_{An}) according to:

$$\Phi_{An} = \frac{S_{An}}{S_{Rho}} \frac{\varepsilon_{Rho}}{\varepsilon_{An}} \Phi_{Rho} \quad (1)$$

As a control, similar analyses were performed on isorhodopsin and 13-desmethyl rhodopsin. According to our regeneration experiments, the molar extinction coefficients of the pigment analogs are within 10% of the rhodopsin value (see above) and equation (1) was used in a simplified form:

$$\Phi_{An} = \frac{S_{An}}{S_{Rho}} \Phi_{Rho} \quad (2)$$

The molar absorbance coefficient of rhodopsin (ε_{Rho}) is 40,600(±500) M^{-1} cm^{-1} at 498 nm (λ_{max}). The molar absorbance coefficient of isorhodopsin (ε_{Iso}) is 43,000 M^{-1} cm^{-1} at λ_{max} (485 nm), but at the excitation wavelengths it is close to that of rhodopsin.[80]

FTIR spectroscopy

FTIR analyses were performed with a Bruker IFS 66/S spectrometer equipped with a liquid nitrogen-cooled,

narrow-band HgCdTe (MCT) detector. Spectra were taken at 2 cm^{-1} resolution. The sample temperature was computer-controlled using a variable temperature, helium-cooled cryostat (Heliostat, APD cryogenics Inc.) covered with a set of NaCl windows in the IR light path. Membrane films of the samples were prepared by isopotential spin drying of 1–2 nmol of pigment on AgCl windows (Crystran Limited, UK),[81] which were subsequently rehydrated with buffer A and sealed using a second AgCl window and a rubber O-ring spacer.[82] Samples were illuminated in the spectrometer using a modified (150W halogen) fiber optics ring illuminator (Schott) equipped with a 488(±10) nm interference filter (Schott) and a set of long-pass filters. Generally, six spectra of the dark-state receptor of 1280 scans each with 120 s acquisition time per spectrum were taken and summed. Subsequently, following 300 s illumination through the 488 nm filter, spectra of the photo-intermediate were taken. Difference spectra were calculated by subtracting the spectrum of rhodopsin from the spectrum of the photo-intermediate. For analysis of the first photoproduct (Batho in native rhodopsin), the sample temperature was kept at 80.0(±0.2) K. Photoreversal of this intermediate to the rhodopsin state was attempted by illuminating the sample for 300 s with light of $\lambda > 610$ nm (Schott RG610 long-pass filter) or $\lambda > 530$ nm (Schott GG530 long-pass filter). Following photo-intermediates were examined at 253 K and 283 K, since at these temperatures the Meta-I intermediate and the active state (Meta-II intermediate) of rhodopsin, respectively, are sufficiently stable to allow the analysis.

Signaling activity

Activation of the rhodopsin-associated G protein transducin was monitored using a fluorescence assay as described.[83,84] The intrinsic fluorescence of activated bovine transducin is enhanced upon binding of GTP, which was recorded on a Shimadzu RF-5301PC spectrofluorimeter (excitation 295 nm; bandwidth 1.5 nm; emission 337 nm; bandwidth 15 nm). Measurements were performed at pH 7.4 and 20 °C with about 100 nM transducin and 5 nM pigment in a buffer containing 20 mM HEPPS, 100 mM NaCl, 2 mM $MgCl_2$, 1 mM dithioerythritol, and 0.01% (w/v) dodecyl-1-β-maltoside at a final volume of 2 ml. A hypotonic extract of isotonically washed rod outer segments served as the source for transducin.[85] Immediately before data acquisition, the reaction mixture was bleached for 300 s in bright white light. After reaching a steady fluorescence level, GTP-γ-S (Boehringer Mannheim) was added to a final concentration of 2.5 μM and the subsequent increase in tryptophan fluorescence of the α-subunit of transducin ($G_t\alpha$) was monitored. In every set of measurements, rhodopsin was included as a 100% control. Opsin membranes served as a negative control. Initial rates were calculated and converted into a percentage of the activation rate achieved by rhodopsin.

Acknowledgements

We acknowledge the assistance of Arthur Pistorius (RUNMC) with assigning vibrational bands in the FTIR spectra.

References

1. Wald, G. (1968). The molecular basis of visual excitation. *Nature*, **219**, 800–807.
2. Hofmann, K. P. (2000). Late photoproducts and signaling states of bovine rhodopsin. In *Molecular Mechanisms in Visual Transduction* (Stavenga, D. G., DeGrip, W. J. & Pugh, E. N., Jr, eds), pp. 91–142, Elsevier Science Publisher, Amsterdam.
3. Verdegem, P. J. E., Helmle, M., Lugtenburg, J. & DeGroot, H. J. M. (1997). Internuclear distance measurements up to 0.44 nm for retinals in the solid state with 1-D rotational resonance ^{13}C MAS NMR spectroscopy. *J. Am. Chem. Soc.* **119**, 169–174.
4. Verdegem, P. J. E., Bovee-Geurts, P. H. M., DeGrip, W. J., Lugtenburg, J. & DeGroot, H. J. M. (1999). Retinylidene ligand structure in bovine rhodopsin, metarhodopsin I, and 10-methylrhodopsin from internuclear distance measurements using ^{13}C-labeling and 1-D rotational resonance MAS NMR. *Biochemistry-USA*, **38**, 11316–11324.
5. Okada, T., Sugihara, M., Bondar, A.-N., Elstner, M., Entel, P. & Buss, V. (2004). The retinal conformation and its environment in rhodopsin in light of a new 2.2 Å crystal structure. *J. Mol. Biol.* **342**, 571–583.
6. Bifone, A., DeGroot, H. J. M. & Buda, F. (1997). Ab initio molecular dynamics of rhodopsin. *Pure Appl. Chem.* **69**, 2105–2110.
7. Cembran, A., Bernardi, F., Olivucci, M. & Garavelli, M. (2005). The retinal chromophore/chloride ion pair: structure of the photo-isomerization path and interplay of charge transfer and covalent states. *Proc. Natl Acad. Sci. USA*, **102**, 6255–6260.
8. Mathies, R. A. & Lugtenburg, J. (2000). The primary photoreaction of rhodopsin. In *Molecular Mechanisms in Visual Transduction* (Stavenga, D. G., DeGrip, W. J. & Pugh, E. N., Jr, eds), pp. 55–90, Elsevier Science Publisher, Amsterdam.
9. Yan, E. C. Y., Ganim, Z., Kazmi, M. A., Chang, B. S. W., Sakmar, T. P. & Mathies, R. A. (2004). Resonance Raman analysis of the mechanism of energy storage and chromophore distortion in the primary visual photoproduct. *Biochemistry-USA*, **43**, 10867–10876.
10. Kukura, P., McCamant, D. W., Yoon, S., Wandschneider, D. B. & Mathies, R. A. (2005). Structural observation of the primary isomerization in vision with femtosecond-stimulated Raman. *Science*, **310**, 1006–1009.
11. Nakamichi, H. & Okada, T. (2006). Crystallographic analysis of primary visual photochemistry. *Angew. Chem. Int. Ed.* **45**, 4270–4273.
12. Kliger, D. S. & Lewis, J. W. (1995). Spectral and kinetic characterization of visual pigment photointermediates. *Isr. J. Chem.* **35**, 309–323.
13. Kochendoerfer, G. G., Verdegem, P. J. E., VanDerHoef, I., Lugtenburg, J. & Mathies, R. A. (1996). Retinal analog study of the role of steric interactions in the excited state isomerization dynamics of rhodopsin. *Biochemistry-USA*, **35**, 16230–16240.
14. Ganter, U. M., Gärtner, W. & Siebert, F. (1990). The influence of the 13-methyl group of the retinal on the photoreaction of rhodopsin revealed by FTIR difference spectroscopy. *Eur. Biophys. J.* **18**, 295–299.
15. Ganter, U. M., Schmid, E. D., Perez-Sala, D., Rando, R. R. & Siebert, F. (1989). Removal of the 9-methyl group of retinal inhibits signal transduction in the visual process. A Fourier-transform infrared and biochemical investigation. *Biochemistry-USA*, **28**, 5954–5962.

16. Meyer, C. K., Böhme, M., Ockenfels, A., Gärtner, W., Hofmann, K. P. & Ernst, O. P. (2000). Signaling states of rhodopsin - Retinal provides a scaffold for activating proton transfer switches. *J. Biol. Chem.* **275**, 19713–19718.
17. Kropf, A., Whittenberger, B. P., Goff, S. P. & Waggoner, A. S. (1973). The spectral properties of some visual pigment analogs. *Expt. Eye Res.* **17**, 591–606.
18. Vogel, R., Fan, G.-B., Sheves, M. & Siebert, F. (2000). The molecular origin of the inhibition of transducin activation in rhodopsin lacking the 9-methyl group of the retinal chromophore: a UV-Vis and FTIR spectroscopic study. *Biochemistry-USA*, **39**, 8895–8908.
19. Ebrey, T. G., Tsuda, M., Sassenrath, G., West, J. L. & Waddell, W. H. (1980). Light activation of bovine rod phosphodiesterase by non-physiological visual pigments. *FEBS Letters*, **116**, 217–219.
20. Corson, D. W., Kefalov, V. J., Cornwall, M. C. & Crouch, R. K. (2000). Effect of 11-cis 13-demethylretinal on phototransduction in bleach-adapted rod and cone photoreceptors. *J. Gen. Physiol.* **116**, 283–297.
21. Corson, D. W., Cornwall, M. C., MacNichol, E. F., Jr, Tsang, S. H., Derguini, F., Crouch, R. K. & Nakanishi, K. (1994). Relief of opsin desensitization and prolonged excitation of rod photoreceptors by 9-desmethylretinal. *Proc. Natl Acad. Sci. USA*, **91**, 6958–6962.
22. Vogel, R., Lüdeke, S., Siebert, F., Sakmar, T. P., Hirshfeld, A. & Sheves, M. (2006). Agonists and partial agonists of rhodopsin: Retinal polyene methylation affects receptor activation. *Biochemistry-USA*, **45**, 1640–1652.
23. DeLange, F., Bovee-Geurts, P. H. M., VanOostrum, J., Portier, M. D., Verdegem, P. J. E., Lugtenburg, J. & DeGrip, W. J. (1998). An additional methyl group at the 10-position of retinal dramatically slows down the kinetics of the rhodopsin photocascade. *Biochemistry-USA*, **37**, 1411–1420.
24. Einterz, C. M., Hug, S. J., Lewis, J. W. & Kliger, D. S. (1990). Early photolysis intermediates of the artificial visual pigment 13-demethylrhodopsin. *Biochemistry-USA*, **29**, 1485–1491.
25. Liu, R. S. H., Crescitelli, F., Denny, M., Matsumoto, H. & Asato, A. E. (1986). Photosensitivity of 10-substituted visual pigment analogues: Detection of a specific secondary opsin-retinal interaction. *Biochemistry-USA*, **25**, 7026–7030.
26. Liu, R. S. H., Asato, A. E., Denny, M. & Mead, D. A. (1984). The nature of restrictions in the binding site of rhodopsin. A model study. *J. Amer. Chem. Soc.* **106**, 8298–8300.
27. Liu, R. S. H. & Asato, A. E. (1990). The binding site of opsin based on analog studies with isomeric, fluorinated, alkylated, and other modified retinals. In *Chemistry and Biology of Synthetic Retinoids* (Dawson, M. I. & Okamura, W. H., eds), pp. 52–75, CRC Press, Boca Raton, FL.
28. Bifone, A., DeGroot, H. J. M. & Buda, F. (1997). Energy storage in the primary photoproduct of vision. *J. Phys. Chem. B*, **101**, 2954–2958.
29. Buda, F., DeGroot, H. J. M. & Bifone, A. (1996). Charge localization and dynamics in rhodopsin. *Phys. Rev. Letters*, **77**, 4474–4477.
30. DeGrip, W. J. & Rothschild, K. J. (2000). Structure and mechanism of vertebrate visual pigments. In *Molecular Mechanisms in Visual Transduction* (Stavenga, D. G., DeGrip, W. J. & Pugh, E. N., Jr, eds), pp. 1–54, Elsevier Science Publisher, Amsterdam.
31. Kim, J. E., Pan, D. H. & Mathies, R. A. (2003). Picosecond dynamics of G-protein coupled receptor activation in rhodopsin from time-resolved UV resonance Raman spectroscopy. *Biochemistry-USA*, **42**, 5169–5175.
32. Pan, D. H., Ganim, Z., Kim, J. E., Verhoeven, M. A., Lugtenburg, J. & Mathies, R. A. (2002). Time-resolved resonance Raman analysis of chromophore structural changes in the formation and decay of rhodopsin's BSI intermediate. *J. Am. Chem. Soc.* **124**, 4857–4864.
33. Pan, D. H. & Mathies, R. A. (2001). Chromophore structure in lumirhodopsin and metarhodopsin I by time-resolved resonance Raman microchip spectroscopy. *Biochemistry-USA*, **40**, 7929–7936.
34. Cooper, A. (1981). Rhodopsin photoenergetics–lumirhodopsin and the complete energy profile. *FEBS Letters*, **123**, 324–326.
35. Cooper, A. (1979). Energy uptake in the first step of visual excitation. *Nature*, **282**, 531–533.
36. DeGrip, W. J., Gray, D., Gillespie, J., Bovee-Geurts, P. H. M., VanDenBerg, E. M. M., Lugtenburg, J. & Rothschild, K. J. (1988). Photoexcitation of rhodopsin: conformation changes in the chromophore, protein and associated lipid, as determined by FTIR difference spectroscopy. *Photochem. Photobiol.* **48**, 497–504.
37. Rothschild, K. J., Cantore, W. A. & Marrero, H. (1983). Fourier transform infrared difference spectra of intermediates in rhodopsin bleaching. *Science*, **219**, 1333–1335.
38. Han, M., Groesbeek, M., Smith, S. O. & Sakmar, T. P. (1998). Role of the C9 methyl group in rhodopsin activation: characterization of mutant opsins with the artificial chromophore 11-cis-9-demethylretinal. *Biochemistry-USA*, **37**, 538–545.
39. Rodieck, R. W. (1973). *The Vertebrate Retina - Principles of Structure and Function.* W.H. Freeman and Company, San Francisco, CA.
40. Sperling, W. & Rafferty, C. N. (1969). Relationship between absorption spectrum and molecular conformations of 11-*cis*-retinal. *Nature*, **224**, 590–594.
41. Tsujimoto, K., Shirasaka, Y., Mizukami, T. & Ohashi, M. (1997). Unusual conformation and photoisomerization of retinochrome analogues with 11-methylretinals. *Chem. Letters*, 813–814.
42. Wang, Y.-J., Bovee-Geurts, P. H. M., Lugtenburg, J. & DeGrip, W. J. (2004). Constraints of the 9-methyl group binding pocket of the rhodopsin chromophore probed by 9-halogeno substitution. *Biochemistry-USA*, **43**, 14802–14810.
43. Palczewski, K., Kumasaka, T., Hori, T., Behnke, C. A., Motoshima, H., Fox, B. A. *et al.* (2000). Crystal structure of rhodopsin: a G protein-coupled receptor. *Science*, **289**, 739–745.
44. Sheves, M., Albeck, A., Ottolenghi, M., Bovee-Geurts, P. H. M., DeGrip, W. J., Einterz, C. M. *et al.* (1986). An artifical visual pigment with restricted C9-C11 motion forms normal photolysis intermediates. *J. Am. Chem. Soc.* **108**, 6440–6441.
45. Asato, A. E., Denny, M. & Liu, R. S. H. (1986). Bioorganic studies of visual pigment analogs. 5. Retinal and rhodopsin analogs directed toward a better understanding of the H.T.-*n* model of the primary process of vision. *J. Am. Chem. Soc.* **108**, 5032–5033.
46. Eyring, G., Curry, B., Broek, A., Lugtenburg, J. & Mathies, R. A. (1982). Assignment and interpretation of hydrogen out-of-plane vibrations in the resonance Raman spectra of rhodopsin and bathorhodopsin. *Biochemistry-USA*, **21**, 384–393.
47. Mathies, R. A., Smith, S. O. & Palings, I. (1987). Determination of retinal chromophore structure in

rhodopsins. In *Resonance Raman Spectra of Polyenes and Aromatics* (Spiro, T. G., ed), pp. 59–108, John Wiley and Sons, New York, NY.
48. Touw, S. I. E., DeGroot, H. J. M. & Buda, F. (2004). Ab initio modeling of the spatial, electronic, and vibrational structure of Schiff base models for visual photoreceptors. *J. Phys. Chem. B*, **108**, 13560–13572.
49. Palings, I., Pardoen, J. A., VanDenBerg, E. M. M., Winkel, C., Lugtenburg, J. & Mathies, R. A. (1987). Assignment of fingerprint vibrations in the resonance Raman spectra of rhodopsin, isorhodopsin, and bathorhodopsin: implications for chromophore structure and environment. *Biochemistry-USA*, **26**, 2544–2556.
50. Palings, I., VanDenBerg, E. M. M., Lugtenburg, J. & Mathies, R. A. (1989). Complete assignment of the hydrogen out-of-plane wagging vibrations of bathorhodopsin: Chromophore structure and energy storage in the primary photoproduct of vision. *Biochemistry-USA*, **28**, 1498–1507.
51. Wang, Q., Kochendoerfer, G. G., Schoenlein, R. W., Verdegem, P. J. E., Lugtenburg, J., Mathies, R. A. & Shank, C. V. (1996). Femtosecond spectroscopy of a 13-demethylrhodopsin visual pigment analogue: The role of non-bonded interactions in the isomerization process. *J. Phys. Chem. B*, **100**, 17388–17394.
52. Parkes, J. H. & Liebman, P. A. (1984). Temperature and pH dependence of the Metarhodopsin I-Metarhodopsin II kinetics and equilibria in bovine rod disk membrane suspensions. *Biochemistry-USA*, **23**, 5054–5061.
53. Matthews, R. G., Hubbard, R., Brown, P. K. & Wald, G. (1963). Tautomeric forms of metarhodopsin. *J. Gen. Physiol.* **47**, 215–240.
54. Kolesnikov, A. V., Golobokova, E. Y. & Govardovskii, V. I. (2003). The identity of metarhodopsin III. *Visual Neurosci.* **20**, 249–265.
55. Kusnetzow, A. K., Altenbach, C. & Hubbell, W. L. (2006). Conformational states and dynamics of rhodopsin in micelles and bilayers. *Biochemistry-USA*, **45**, 5538–5550.
56. Vogel, R., Siebert, F., Zhang, X. Y., Fan, G.-B. & Sheves, M. (2004). Formation of meta III during the decay of activated rhodopsin proceeds via meta I and not via meta. *Biochemistry-USA*, **43**, 9457–9466.
57. Vogel, R., Siebert, F., Lüdeke, S., Hirshfeld, A. & Sheves, M. (2005). Agonists and partial agonists of rhodopsin: Retinals with ring modifications. *Biochemistry-USA*, **44**, 11684–11699.
58. Bartl, F. J., Fritze, O., Ritter, E., Herrmann, R., Kuksa, V., Palczewski, K. *et al.* (2005). Partial agonism in a G protein-coupled receptor - role of the retinal ring structure in rhodopsin activation. *J. Biol. Chem.* **280**, 34259–34267.
59. DeLange, F., Bovee-Geurts, P. H. M., Pistorius, A. M. A., Rothschild, K. J. & DeGrip, W. J. (1999). Probing intramolecular orientations in rhodopsin and metarhodopsin II by polarized infrared difference spectroscopy. *Biochemistry-USA*, **38**, 13200–13209.
60. Spooner, P. J. R., Sharples, J. M., Goodall, S. C., Bovee-Geurts, P. H. M., Verhoeven, M. A., Lugtenburg, J. *et al.* (2004). The ring of the rhodopsin chromophore in a hydrophobic activation switch within the binding pocket. *J. Mol. Biol.* **343**, 719–730.
61. Patel, A. B., Crocker, E., Eilers, M., Hirshfeld, A., Sheves, M. & Smith, S. O. (2004). Coupling of retinal isomerization to the activation of rhodopsin. *Proc. Natl Acad. Sci. USA*, **101**, 10048–10053.
62. Verhoeven, M. A. (2005). Electronic and spatial characteristics of the retinylidene chromophore of rhodopsin. PhD Thesis, Leiden University, The Netherlands.
63. Liu, R. S. H. & Colmenares, L. U. (2003). The molecular basis for the high photosensitivity of rhodopsin. *Proc. Natl Acad. Sci. USA*, **100**, 14639–14644.
64. Birge, R. R. & Vought, B. W. (2000). Energetics of rhodopsin photobleaching: photocalorimetric studies of energy storage in early and later intermediates. *Methods Enzymol.* **315**, 143–163.
65. Wang, Y.-J. & Lugtenburg, J. (2004). Preparation of (*all-E*)- and (*11Z*)-12-haloretinals and (*11Z,13Z*)- and (*13Z*)-14-haloretinals by the C_{15}+C_5 route - exploring the possibility of preparing any retinoid rationally chemically modified at any position in the conjugated tail. *Eur. J. Org. Chem.* 5100–5110.
66. Schick, G. A., Cooper, T. M., Holloway, R. A., Murray, L. P. & Birge, R. R. (1987). Energy-storage in the primary photochemical events of rhodopsin and isorhodopsin. *Biochemistry-USA*, **26**, 2556–2562.
67. Kim, J. E., Tauber, M. J. & Mathies, R. A. (2001). Wavelength dependent cis-trans isomerization in vision. *Biochemistry-USA*, **40**, 13774–13778.
68. Creemers, A. F. L. & Lugtenburg, J. (2002). The preparation of all-trans uniformly ^{13}C-labeled retinal via a modular total organic synthetic strategy. Emerging central contribution of organic synthesis toward the structure and function study with atomic resolution in protein research. *J. Am. Chem. Soc.* **124**, 6324–6334.
69. Lugtenburg, J. (1985). The synthesis of ^{13}C-labeled retinals. *Pure Appl. Chem.* **57**, 753–762.
70. Groesbeek, M., Rood, G. A. & Lugtenburg, J. (1992). Synthesis of (12,13-$^{13}C_2$)retinal and (13,14-$^{13}C_2$)retinal - a strategy to prepare multiple-^{13}C-labeled conjugated systems. *Rec. Trav. Chim. J. Roy. Neth. Chem.* **111**, 149–154.
71. Olivè, J.-L., Mousseron-Canet, M. & Dornand, J. (1969). Acetylenic intermediates in synthesis of vitamin A and its isomers. *Bull. Soc. Chim. Fr.*, 3247–3252.
72. Jansen, F.-J. H. M., Kwestro, M., Schmitt, D. & Lugtenburg, J. (1994). Synthesis and characterization of all-E (*12,12′*-$^{13}C_2$)astaxanthin, (*13,13′*-$^{13}C_2$)astaxanthin, (*14,14′*-$^{13}C_2$)astaxanthin, (*15,15′*-$^{13}C_2$)astaxanthin and (*20,20′*-$^{13}C_2$)astaxanthin. *Rec. Trav. Chim. J. Roy. Neth. Chem.* **113**, 552–562.
73. Sato, K., Mizuno, S. & Hirayama, M. (1967). A total synthesis of phytol. *J. Org. Chem.* **32**, 177–180.
74. Friese, A., Hell-Momeni, K., Zundorf, I., Winckler, T., Dingermann, T. & Dannhardt, G. (2002). Synthesis and biological evaluation of cycloalkylidene carboxylic acids as novel effectors of Ras/Raf interaction. *J. Med. Chem.* **45**, 1535–1542.
75. Cooke, M. P. (1986). Acylation of organolithium reagents by esters in the presence of chlorotrimethylsilane. *J. Org. Chem.* **51**, 951–953.
76. Hubbard, R., Brown, P. K. & Bownds, M. D. (1971). Methodology of vitamin A and visual pigments. *Methods Enzymol.* **18**, 615–653.
77. DeGrip, W. J., VanOostrum, J., Bovee-Geurts, P. H. M., VanDerSteen, R., VanAmsterdam, L. J. P., Groesbeek, M. & Lugtenburg, J. (1990). 10,20-Methanorhodopsins: (7*E*,9*E*,13*E*)-10,20-methanorhodopsin and (7*E*,9*Z*,13*Z*)-10,20-methanorhodopsin - 11-*cis*-locked rhodopsin analog pigments with unusual thermal and photo-stability. *Eur. J. Biochem.* **191**, 211–220.
78. DeGrip, W. J., VanOostrum, J. & Bovee-Geurts, P. H. M. (1998). Selective detergent-extraction from mixed detergent/lipid/protein micelles, using cyclodextrin inclusion compounds: a novel generic

approach for the preparation of proteoliposomes. *Biochem. J.* **330**, 667–674.
79. Dartnall, H. J. A. (1972). Photosensitivity. In *Photochemistry of Vision* (Dartnall, H. J. A., ed), pp. 122–145, Springer-Verlag, Berlin.
80. Hubbard, R. & Wald, G. (1952). Cis-trans isomers of vitamin A and retinene in the rhodopsin system. *J. Gen. Physiol.* **36**, 269–315.
81. Clark, N. A., Rothschild, K. J., Simon, B. A. & Luippold, D. A. (1980). Surface induced orientation of multilayer membrane arrays: Theoretical analysis and a new method with application to purple membrane fragments. *Biophys. J.* **31**, 65–96.
82. DeLange, F., Merkx, M., Bovee-Geurts, P. H. M., Pistorius, A. M. A. & DeGrip, W. J. (1997). Modulation of the metarhodopsin I/metarhodopsin II equilibrium of bovine rhodopsin by ionic strength - evidence for a surface charge effect. *Eur. J. Biochem.* **243**, 174–180.
83. Phillips, W. J. & Cerione, R. A. (1988). The intrinsic fluorescence of the a subunit of transducin - Measurement of receptor-dependent guanine nucleotide exchange. *J. Biol. Chem.* **263**, 15498–15505.
84. Fahmy, K. & Sakmar, T. P. (1993). Regulation of the rhodopsin-transducin interaction by a highly conserved carboxylic acid group. *Biochemistry-USA*, **32**, 7229–7236.
85. Kühn, H. (1984). Interactions between photoexcited rhodopsin and light-activated enzymes in rods. *Prog. Retin. Res.* **3**, 123–156.

Edited by R. Huber

(Received 10 May 2006; received in revised form 12 July 2006; accepted 19 July 2006)
Available online 28 July 2006